

## STOCHASTIC ROBUSTNESS OF LINEAR CONTROL SYSTEMS

Robert F. Stengel and Laura E. Ryan  
Department of Mechanical and Aerospace Engineering  
Princeton University

### ABSTRACT

A simple numerical procedure for estimating the *stochastic robustness* of a linear, time-invariant system is described. Monte Carlo evaluation of the system's eigenvalues allows the *probability of instability* and the related *stochastic root locus* to be estimated. This definition of robustness is an alternative to existing deterministic definitions that address both structured and unstructured parameter variations directly. This analysis approach treats not only Gaussian parameter uncertainties but non-Gaussian cases, including uncertain-but-bounded variations. Trivial extensions of the procedure admit alternate discriminants to be considered. Thus, the probabilities that stipulated degrees of instability will be exceeded or that closed-loop roots will leave desirable regions also can be estimated. Results are particularly amenable to graphical presentation.

### INTRODUCTION

Control system robustness is defined as the ability to maintain satisfactory stability or performance characteristics in the presence of all conceivable system parameter variations. While assured robustness may be viewed as an alternative to gain adaptation or scheduling to accommodate known parameter variations, more often it is seen as protection against uncertainties in plant specification. Consequently, a statistical description of control system robustness is consistent with what may be known about the structure and parameters of the plant's dynamic model.

Guaranteeing robustness has long been a design objective of control system analysis, although in most instances, insensitivity to parameter variations has been treated as a deterministic problem (see Ref. 1 for a comprehensive presentation of both classical and modern robust control). Stability (gain and phase) margins are useful concepts for designing robust single-input/single-output systems, addressing disturbance rejection and other performance goals in the process, and they are amenable to the manual graphical procedures that preceded the widespread use of computers. With the help of these computers, singular-value analysis has extended the frequency-domain approach to multi-input/multi-output systems (e.g., [2,3]); however, guaranteed-stability-bound estimates often are unduly conservative, and the relationship to parameter variations in the physical system is weak. Structured-singular-value analysis [4] reduces this conservatism somewhat, and alternate treatments of structured parameter variations have been proposed (e.g., [5-7]), though these approaches remain deterministic. Elements of stochastic stability [8] have application to robustness but have yet to be presented in that context.

Presented at the 1989 Conference on Information Sciences and Systems, Johns Hopkins University, Baltimore, MD.

The notion of *probability of instability*, which is central to the analysis of stochastic robustness, was introduced in Ref. 9, with application to the robustness of the Space Shuttle's flight control system, and it is further described in Ref. 10. This method determines the *stochastic robustness* of a linear, time-invariant system by the probability distributions of closed-loop eigenvalues, given the statistics of the variable parameters in the plant's dynamic model. The probability that all of these eigenvalues lie in the open left-half  $s$  plane is the scalar measure of robustness.

With the advent of fast graphics workstations and supercomputers, the stochastic robustness of a system is easily computed by Monte Carlo simulation, and results can be displayed pictorially, providing insight into otherwise hidden robustness properties of the system. The method is computationally simple, requiring only matrix manipulation and eigenvalue computation, and it is inherently non-conservative, given a large enough sample space. Furthermore, the analysis of stochastic robustness is a logical adjunct to parameter-space control design methods [11-14]. Details of the approach and examples are given in the sequel.

### PROBABILITY OF INSTABILITY

Consider a linear, time-invariant (LTI) system of the form,

$$\dot{\mathbf{x}}(t) = \mathbf{F}(\mathbf{p})\mathbf{x}(t) + \mathbf{G}(\mathbf{p})\mathbf{u}(t) \quad (1)$$

$$\mathbf{y}(t) = \mathbf{H}(\mathbf{p})\mathbf{x}(t) \quad (2)$$

where  $\mathbf{x}(t)$ ,  $\mathbf{u}(t)$ ,  $\mathbf{y}(t)$ , and  $\mathbf{p}$  are state, control, output, and parameter vectors of dimension  $n$ ,  $m$ ,  $q$ , and  $r$ , respectively, accompanied by conformable dynamic, control, and output matrices  $\mathbf{F}$ ,  $\mathbf{G}$ , and  $\mathbf{H}$ , which may be arbitrary functions of  $\mathbf{p}$ . The plant is subject to LTI control,

$$\mathbf{u}(t) = \mathbf{u}_c(t) - \mathbf{C}\mathbf{H}(\mathbf{p})\mathbf{x}(t) \quad (3)$$

$\mathbf{u}_c(t)$  is a command input vector, and, for simplicity, the ( $m \times n$ ) control gain matrix  $\mathbf{C}$  is assumed to be known without error. The  $n$  eigenvalues,  $\lambda_i = \sigma_i + j\omega_i$ ,  $i = 1$  to  $n$ , of the matrix  $[\mathbf{F}(\mathbf{p}) - \mathbf{G}(\mathbf{p})\mathbf{C}\mathbf{H}(\mathbf{p})]$  determine closed-loop stability and can be determined as the roots of the determinant equation,

$$|s\mathbf{I}_n - [\mathbf{F}(\mathbf{p}) - \mathbf{G}(\mathbf{p})\mathbf{C}\mathbf{H}(\mathbf{p})]| = 0 \quad (4)$$

where  $s$  is a complex operator and  $\mathbf{I}_n$  is the ( $n \times n$ ) identity matrix. System stability requires that no eigenvalues have positive real parts. The relationship between parameters and eigenvalues is complicated.

Even if  $F$ ,  $G$ , and  $H$  are linear functions of  $\mathbf{p}$ , the associations between  $\mathbf{p}$  and the  $\lambda_i$  are nonlinear, and there is the further possibility of products of parameters in the feedback term. Consequently, while small-parameter-variation sensitivities of the eigenvalues can be estimated by linear methods [10], the hopes for generally applicable analytic expressions are slim.

Putting aside the mathematical intricacies, note that the probability of stability plus the probability of instability is one:

$$\Pr(\text{stability}) + \Pr(\text{instability}) = 1 \quad (5)$$

Stochastic robustness is achieved when the probability of stability (instability) is large (small). Since stability requires all the roots to be in the open-left-half  $s$  plane, while instability results from even a single right-half  $s$  plane root, we may write

$$\Pr(\text{instability}) \triangleq \mathbb{P} = 1 - \int_{-\infty}^{\infty} \text{pr}(\sigma) d\sigma \quad (6)$$

where  $\sigma$  is an  $n$ -vector of the real parts of the system's eigenvalues,  $\text{pr}(\sigma)$  is the joint probability density function of  $\sigma$ , and the integral that defines the probability of stability is evaluated over the space of individual components of  $\sigma$ .

Estimating the probability of stability of a closed-loop system from repeated eigenvalue calculation is a straightforward task. Denoting the probability density function of  $\mathbf{p}$  as  $\text{pr}(\mathbf{p})$ , eq. 4 is evaluated  $J$  times with each element of  $\mathbf{p}_j$ ,  $j = 1$  to  $J$ , specified by a random-number generator whose individual outputs are shaped by  $\text{pr}(\mathbf{p})$ . This *Monte Carlo evaluation* of the probability of stability becomes increasingly precise as  $J$  becomes large. Then,

$$\int_{-\infty}^{\infty} \text{pr}(\sigma) d\sigma = \lim_{J \rightarrow \infty} \frac{N(\sigma_{\max} \leq 0)}{J} \quad (7)$$

$N(\cdot)$  is the number of cases for which all elements of  $\sigma$  are less than or equal to zero, that is, for which  $\sigma_{\max} \leq 0$ , where  $\sigma_{\max}$  is the maximum real eigenvalue component in  $\sigma$ . An important feature of this definition is that it does not depend on the eigenvalues and eigenvectors retaining fixed structures. As parameters change, complex roots may coalesce to become real roots (or the reverse), and modes may exchange relative frequencies. The only matter for concern is whether or not all real parts of the eigenvalues remain in the left-half  $s$  plane. The stable space of  $\sigma$  is a hypercube with one corner at the origin and all other corners at various infinite points.

There is, of course, no limitation on admissible specifications for the multivariate  $\text{pr}(\mathbf{p})$ : it may be Gaussian or non-Gaussian, as appropriate. Rayleigh, correlated, and any other well-posed distributions are admissible, the principal challenge being to properly shape (and correlate) the outputs of the random-number

generator. In practice, system parameter uncertainties are most likely to be bounded, as typical quality control procedures eliminate out-of-tolerance devices, and there are physical limitations on component size, weight, shape, etc. The rectangular (uniform) distribution is particularly interesting, as it readily models bounded uncertainty, and it is the default distribution of most algorithms for random-number generation. Given binary distributions for each parameter, in which the elements of  $\mathbf{p}$  take maximum or minimum values with equal probability, the Monte Carlo evaluation reduces to  $2^r$  deterministic evaluations, the result is exact, and the probability associated with each possible value of  $\mathbf{p}$  is  $1/2^r$ . Similarly, the distribution for  $r$  parameters, each of which takes  $w$  values (i.e., for quantized rectangular distributions), can be obtained from  $w^r$  evaluations; the probability of acquiring each value of  $\mathbf{p}$  (for equally probable parameter values) is  $1/w^r$ .

Histograms and cumulative distributions for varying degrees of stability are readily given by the Monte Carlo estimate of  $\int_{-\infty}^{\Sigma} \text{pr}(\sigma) d\sigma$ , where  $\Sigma$  represents a maximum real eigenvalue component, and  $-\infty < \Sigma < \infty$ . The histogram is a plot of  $\frac{N[(\Sigma - \Delta) < \sigma_{\max} \leq \Sigma]}{J}$  vs.  $\Sigma$ ;  $\Delta$  is an increment in  $\Sigma$ ,  $N[\cdot]$  is the number of cases whose maximum real eigenvalue components lie in the increment, and  $J$  is the total number of evaluations. The histogram estimates the *stability probability density function*,  $\text{pr}(\Sigma)$ , which is obtained in the limit for a continuous distribution of  $\Sigma$  as  $\Delta \rightarrow 0$  and  $J \rightarrow \infty$ . The *cumulative probability distribution of stability*,  $\Pr(\Sigma)$ , is similarly estimated and presented as  $\frac{N(\sigma_{\max} \leq \Sigma)}{J}$  vs.  $\Sigma$ , the exact distribution being achieved in the limit as  $J \rightarrow \infty$ . Consequently,

$$\mathbb{P} = 1 - \Pr(0). \quad (8)$$

The regions of varying stability degree are hypercubes in  $\sigma$  space, each with one corner at the  $n$ -vector  $\Sigma = [\Sigma \Sigma \dots \Sigma]^T$  and all remaining corners at appropriate infinite locations.

When has stochastic robustness been achieved? The answer is problem-dependent. In some applications involving bounded parameters, it will be possible to choose  $\mathbf{C}$  such that  $\mathbb{P} = 0$ , and that is a desirable goal; however, if admissible parameter variations are unbounded, if  $\mathbf{C}$  is constrained, or if the rank of  $\mathbf{CH}$  is less than  $n$ , the minimum  $\mathbb{P}$  may be greater than zero.  $\mathbf{C}$  then must be chosen to satisfy performance goals and one of two robustness criteria: minimum  $\mathbb{P}$ , or  $\mathbb{P}$  small enough to meet a reliability specification (e.g., one chance of instability in some large number of realizations).

## STOCHASTIC ROOT LOCUS

While it is not necessary to plot the eigenvalues (or roots) of eq. 4 to determine or portray stochastic

robustness, stochastic root loci provide insight regarding the effects of parameter uncertainty on system stability. Consider, for example, a classical second-order system whose roots are solutions to the equation

$$s^2 + 2\zeta\omega_n s + \omega_n^2 = 0 \quad (9)$$

Suppose that the damping ratio ( $\zeta$ ) and natural frequency ( $\omega_n$ ) are nominally 0.707 and 1, respectively, and that each may be a Gaussian-distributed random variable with standard deviation of 0.2. Allowing first  $\zeta$  to vary, then  $\omega_n$ , 100-sample scatter plots of the roots are obtained (Fig. 1). These root loci are immediately recognized as following the classical configurations of root locus construction [15], with the heaviest density of roots in the vicinities of the nominal values. The density of roots depicts the likelihood that eigenvalues vary from their nominal values if either damping ratio or natural frequency is uncertain. These stochastic root loci include branches on the real axis and in the right-half  $s$  plane for large enough variations of  $\zeta$  and  $\omega_n$ .

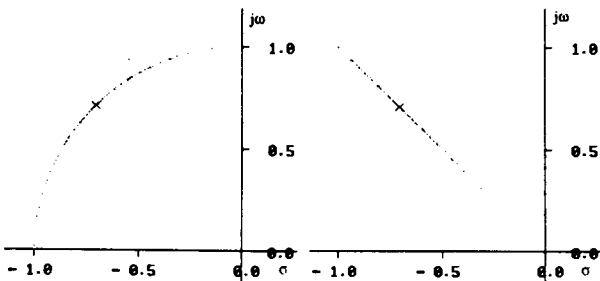


Figure 1. Stochastic root loci of a second-order system with Gaussian damping ratio or natural frequency.  $\zeta_0 = 0.707$ ,  $\omega_{n0} = 1$ ; 100 Monte Carlo evaluations.

- a) Effect of  $\zeta$  variation with 0.2 standard deviation.
- b) Effect of  $\omega_n$  variation with 0.2 standard deviation.

If both  $\zeta$  and  $\omega_n$  are uncertain and uncorrelated (i.e.,  $\mathbf{p} = [\zeta \ \omega_n]^T$ ), the scatter plots become "clouds" surrounding the nominal values; Fig. 2a is one representation of the resulting stochastic root locus based on the calculation of 4,000 samples. Further understanding can be gained by plotting the density of roots in a third dimension above the root locus plot. This is done in two steps. The first step is to divide the  $s$  plane into subspaces (or "bins"), as in Fig. 2b, and to count the number of roots in each bin as a sampled estimate of the root density  $\rho$ . The result is a multivariate histogram, with  $\sigma$  and  $\omega$  serving as independent variables. Complex root bins are elemental areas, for which  $\rho_A$  is defined in units of roots/unit area. Real root bins are confined to the real axis; hence,  $\rho_L$  measures roots/unit length.

The second step is to portray the root density distribution. This can be done by brightening or darkening the bin outlines (Fig. 2b), graphing contours of equal root density on the two-dimensional plot, or by plotting an oblique view of the three-dimensional histogram or root density surface, as in Fig. 2c. The plotted surfaces would become smoother as the number of evaluations increased.

Numerical smoothing also can be applied (judiciously) to account for sampling effects on the plotted surface. For this paper, the graphical presentations are relatively crude, but it is apparent that more sophisticated graphical processing, including the use of false color, hidden-line removal, surface generation, and shading can be applied to good effect. Root densities along the real axis present a special problem for 2-D presentation, in that their distributions are linear, not areal; oblique 3-D views provide a satisfactory alternative.

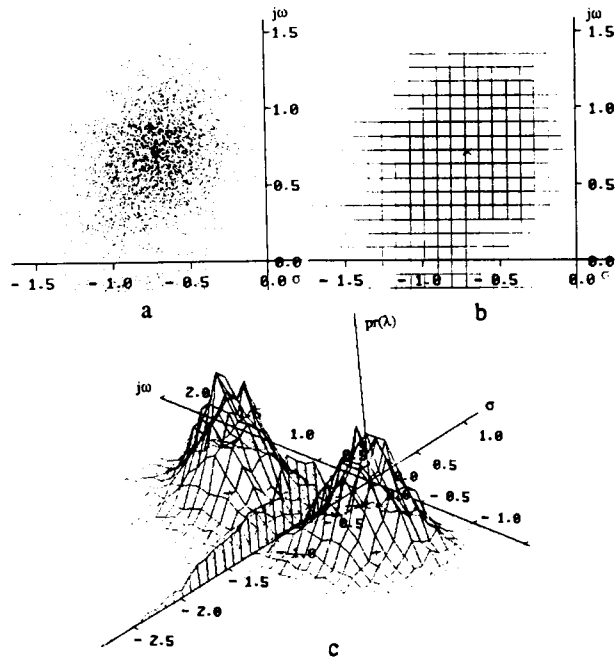


Figure 2. Stochastic root loci of a second-order system with Gaussian damping ratio and natural frequency.  $\zeta_0 = 0.707$ ,  $\omega_{n0} = 1$ ; 4,000 Monte Carlo evaluations.

- a) Scatter plot.
- b) 2-dimensional binned representation.
- c) Oblique 3-dimensional representation.

There is an ostensible relationship between  $\text{pr}(\Sigma)$  and  $\rho$ ; however, the relationship may be multivalued and ambiguous. When considering instability, distinction must be made between the number of cases with right-half-plane roots and the number of roots in the right-half plane. For example, a third-order system with a complex pair of roots and a real root can be unstable with 1, 2, or 3 roots in the right-half plane, yet  $N$  would be incremented by one in each case. A high-order system with real roots could be unstable with one or more roots in the same right-half-plane bin. Again,  $N$  would be incremented by one, although the bin's  $\rho$  depends upon the number of roots it contains.

### A STOCHASTIC ROBUSTNESS EXAMPLE

Reference 16 provides a linear-quadratic-Gaussian (LQG) design problem with a closed-loop system that is nominally stable, but whose stability margins become vanishingly small as control and estimation gains become

large. That example is used here for a demonstration of stochastic stability robustness. An unstable second-order plant,

$$\begin{bmatrix} \dot{x}_1 \\ \dot{x}_2 \end{bmatrix} = \begin{bmatrix} 1 & 1 \\ 0 & 1 \end{bmatrix} \begin{bmatrix} x_1 \\ x_2 \end{bmatrix} + \begin{bmatrix} 0 \\ 1 \end{bmatrix} u + \begin{bmatrix} 1 \\ 1 \end{bmatrix} w \quad (10)$$

$$z = [1 \ 0] \begin{bmatrix} x_1 \\ x_2 \end{bmatrix} + n \quad (11)$$

is to be stabilized by an LQG regulator with controller cost function matrices,

$$Q = Q \begin{bmatrix} 1 & 1 \\ 1 & 1 \end{bmatrix}, \quad R = R = 1 \quad (12,13)$$

and disturbance and measurement-error spectral density matrices

$$W = W \begin{bmatrix} 1 & 1 \\ 1 & 1 \end{bmatrix}, \quad N = N = 1 \quad (14,15)$$

The corresponding LQG control and estimator gains,  $C$  and  $K$ , are [16]

$$C = (2 + \sqrt{4 + Q}) [1 \ 1] = [c \ c] \quad (16)$$

$$K = (2 + \sqrt{4 + W}) [1 \ 1]^T = [k \ k]^T \quad (17)$$

If the actual control effect matrix is  $G = [0 \ \mu]^T$  rather than  $[0 \ 1]^T$ , eq. 4 can be expressed for this problem (with the state consisting of the original state and its estimate,  $x^T = [x_1 \ x_2 \ \hat{x}_1 \ \hat{x}_2]$ ), as,

$$\begin{vmatrix} (s-1) & -1 & 0 & 0 \\ 0 & (s-1) & \mu c & \mu c \\ -k & 0 & (s-1+k) & -1 \\ -k & 0 & (c+k) & (s-1+c) \end{vmatrix} = s^4 + c_3 s^3 + c_2 s^2 + c_1 s + c_0 = 0 \quad (18)$$

Using Routh's criterion, Doyle showed that  $\mu$  remaining in  $(a, b) = \{(1 + 1/ck), [1 - (k + c - 4)/2ck]\}$  is a necessary condition for stability to be retained [17].

Consider two cases with different LQG gains. In Case 1,  $c = k = 4$  (the limiting case as  $Q$  and  $W$  approach zero), and in Case 2,  $c = k = 100$ . Because

$$c_1 = k + c - 4 + 2(\mu-1)ck, \quad c_0 = 1 + (1-\mu)ck \quad (19,20)$$

the characteristic polynomial can be expressed as

$$s^4 + c_3 s^3 + c_2 s^2 + (k+c-4-2ck)s + (1+ck) + \mu ck(2s-1) = 0 \quad (21)$$

which is a root-locus problem with  $\mu ck$  taken as the gain. The nominal roots are found with  $\mu = 1$ , and they are

$$\text{Case 1} \quad \lambda_{1-4} = -1, -1, -1, -1 \quad (22)$$

$$\text{Case 2} \quad \lambda_{1-4} = -0.01, -0.01, -98, -98 \quad (23)$$

Three features are immediately evident. The root locus gain is proportional to  $ck$ ; hence,  $\mu$  has a greater effect on the root locus in the latter case. There is a transmission zero at  $+1/2$  that will draw one root into the right half plane. The excess of poles over zeros is three, indicating that additional instability must occur for large magnitudes of  $(\mu - 1)$ . There will be either one or two unstable roots among those going to infinity, depending on the sign of  $(\mu - 1)$ .

The stochastic root locus plots based on 3,500 Monte Carlo evaluations with  $p = \mu$  corroborate these predictions (Fig. 3). It is assumed that  $\mu$  is a Gaussian random variable with mean equalling  $(a + b)/2$ , representing a bias from the nominal  $\mu$  used to determine the gains, and standard deviation of  $(b - a)/2$ . In both cases, the root distributions are skewed and/or multimodal, and each of the branches has a pronounced peak. Few roots lie near breakaway points, but rather accumulate nearer to the transmission zero or infinity. Figure 3a shows three of the five possible unstable branches, while for the higher gain, only two branches reach instability. Figure 4 indicates that the resulting  $\text{Pr}(\Sigma)$  are non-Gaussian. The corresponding probabilities of instability  $P$  are 0.48 and 0.33, indicating that the resulting distributions are dissimilar, even though the standard deviations were equally scaled for each case. (When the Case 1 standard deviation is used with Case 2's gains,  $P$  climbs to 0.96.)

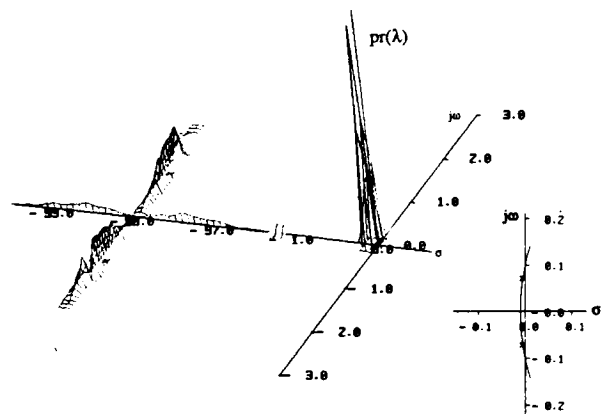
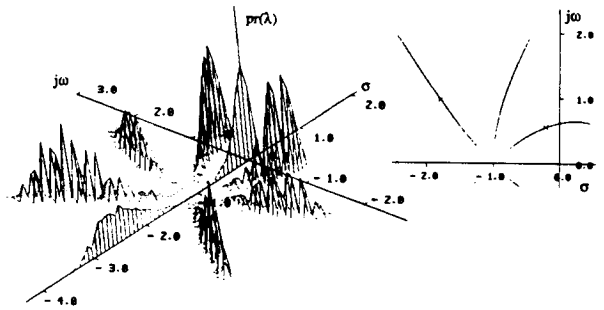


Figure 3. Stochastic root loci for the Doyle LQG counterexample. Gaussian parameter uncertainty with mean  $= (a + b)/2$  and standard deviation  $= (b - a)/2$ .

a)  $c = k = 4$ , b)  $c = k = 100$

ORIGINAL PAGE IS  
OF POOR QUALITY

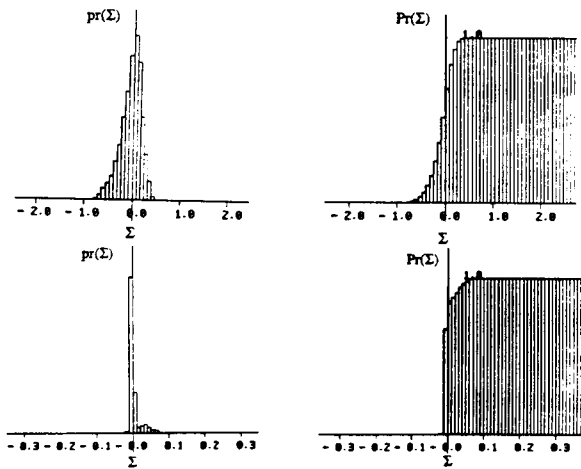


Figure 4. Histograms and cumulative probability distributions for the Doyle LQG counterexample. Gaussian parameter uncertainty with mean =  $(a + b)/2$  and standard deviation =  $(a - b)/2$ .  
a)  $c = k = 4$ , b)  $c = k = 100$

Now consider two similar cases in which  $\mu$  is a random variable with uniform probability in  $(a, b)$ . For Case 1, Figures 5 and 6 illustrate how the stochastic root locus and probability distributions are bounded in comparison with Fig. 3a and 4a. In this example, the bounds given by Routh's criterion are not the actual stability bounds, and the probability of instability  $P$  is non-zero. For Cases 1 and 2, the probabilities of instability  $P$  decrease to 0.27 and 0.01, respectively, as some unstable values associated with the tails of the  $\mu$  distribution have been eliminated. Naturally, if  $\mu$  had been uniformly distributed just inside the actual stability boundaries ( $0.9243 < \mu < 1.0625$ , for  $c = 4$ ),  $P$  would be zero.

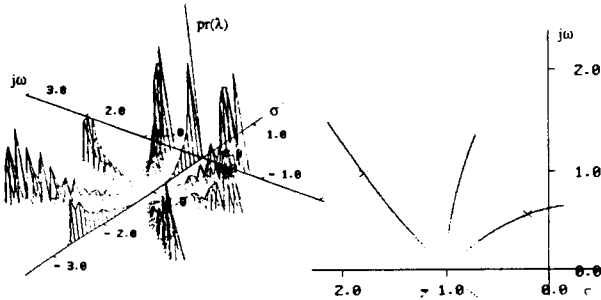


Figure 5. Stochastic root locus for the Doyle LQG counterexample,  $c = k = 4$ . Parameter uniformly distributed in  $(a, b) = (0.875, 1.0625)$ .

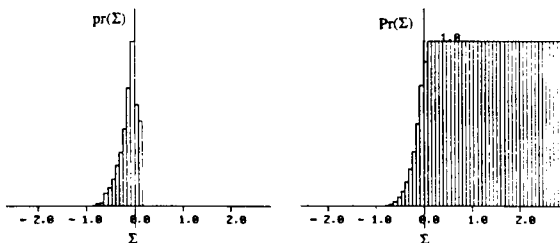


Figure 6. Histogram and cumulative probability distribution for the Doyle LQG counterexample,  $c = k = 4$ . Parameter uniformly distributed in  $(a, b) = (0.875, 1.0625)$

Using Loop Transfer Recovery (LQG/LTR) [17], linear-quadratic (LQ) robustness can be fully recovered. Recovery as a function of design parameter  $v$  ( $W = vW_0$ ) for Case 1 is illustrated in Fig. 7 through both singular-value analysis and the stochastic root locus. The LQG return difference function in this case is a scalar, and the singular value is identically the return difference function:

$$1+a(s) = I + C[sI - (F - GC - KH)]^{-1}KH[sI - F]^{-1}G \quad (24)$$

The original LQ stability margins are not fully recovered until  $v > 10,000$  (Fig 7a). Figure 7b illustrates the mechanism of recovery: increasing  $v$  pushes two eigenvalues to higher frequencies and decreases the variation in the two roots near the origin. Based upon 3,500 evaluations and a Gaussian  $\mu$  variation, the present analysis estimates  $P$  to be zero when  $v \geq 100$ .

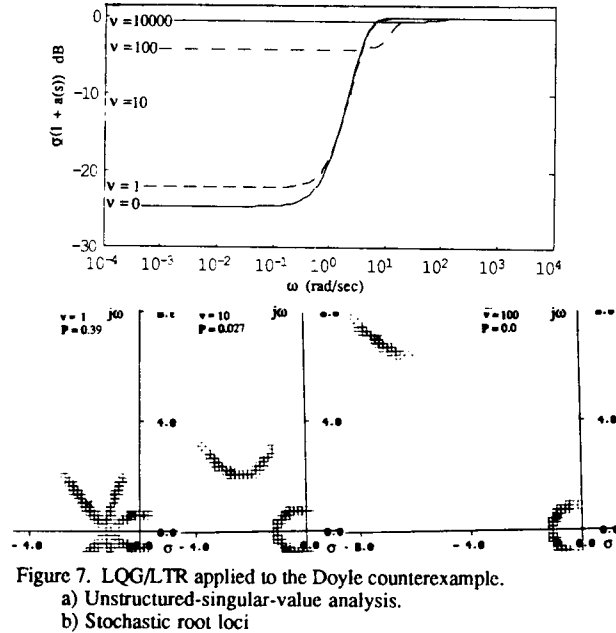


Figure 7. LQG/LTR applied to the Doyle counterexample.  
a) Unstructured-singular-value analysis.  
b) Stochastic root loci

### COMPUTATIONAL ISSUES

The validity of the Monte Carlo analysis is dependent on the number of eigenvalues computed, the number of varying parameters, their probability distributions, and required confidence levels. The number of evaluations required can be related to the number of varying parameters by considering uniform probability distributions. Quantized uniform distributions approximate continuous uniform distributions, approaching them in the limit as the numbers of discrete parameter values go to infinity. Given  $n$  Monte Carlo evaluations of a system with  $r$  continuous uniform parameters, the result is, at best, equivalent to results computed deterministically for a system with  $r$  uniform parameters quantized in  $w$  levels, where  $w = n^{1/r}$ . Conversely, the number of evaluations should be of  $O(\alpha w^r)$ , where  $w$  is an acceptable level of parameter quantization, and  $\alpha \gg 1$ . Note that in a 10-parameter case, direct equivalence to

ten parameter quantization levels requires over 10 billion evaluations, while 10,000 evaluations yield results that are equivalent to a quantization level less than three. Work remains to be done in associating small-sample evaluations with confidence levels of the histograms and the resulting probability of instability.

If  $\sigma_{\max}$  is monotonic in the individual elements of  $p$ , then evaluation results for the binary probability distribution denoted by  $(p_{\min}, p_{\max})$  circumscribe results obtained for continuous or quantized distributions with the same limits. In this case, a conservative estimate of  $P$  is provided by the associated  $2^r$  deterministic evaluations based on binary distributions.

Because each Monte Carlo evaluation can be calculated independently, determining stochastic robustness is a task well-suited to parallel computation. Eigenvalue computation speed is linear in the number of processors, and results from separate processors need be consolidated only at the final stage of display.

### CONCLUSIONS

Stochastic robustness offers a rigorous yet straightforward alternative to current metrics for control system robustness that is simple to compute and is unfettered by normally difficult problem statements, such as non-Gaussian statistics, products of parameter variations, and structured uncertainty. The approach answers the question, "How likely is the closed-loop system to fail, given limits of parameter uncertainty?" It makes good use of modern computational and graphic tools, and it is easily related to practical design considerations. The principal difficulty in applying this method to controlled systems is that it is computationally intensive; however, requirements are well within the capabilities of existing computers. The principal advantage of the approach is that it is easily implemented, and results have direct bearing on engineering objectives.

### ACKNOWLEDGMENT

This research has been sponsored by the FAA and the NASA Langley Research Center under Grant No. NGL 31-001-252.

### REFERENCES

- 1) Dorato, P., ed., *Robust Control*, IEEE Press, New York, 1987.
- 2) Sandell, N.R., Jr., ed., "Recent Developments in the Robustness Theory of Multivariable Systems," Office of Naval Research Rep. No. ONR-CR215-271-1F, Aug 1979.
- 3) Lehtomaki, N. A., Sandell, N. R. Jr, and Athans, M., "Robustness Results in Linear-Quadratic-Gaussian Based Multivariable Control Designs," *IEEE Transactions on Automatic Control*, Vol. AC-26, No. 1, pp. 75-93, Feb 1981.
- 4) Doyle, J. C., "Analysis of Feedback Systems with Structured Uncertainties," *IEE Proceedings*, Vol. 129, Part D, No. 6, pp. 242-250, Nov 1982.
- 5) Tahk, M. and Speyer, J.L., "Modeling of Parameter Variations and Asymptotic LQG Synthesis," *IEEE Transactions on Automatic Control*, Vol. AC-32, No. 9, pp. 793-801, Sept 1987.
- 6) Yedavalli, R.K., and Liang, Z., "Reduced Conservatism in Stability Robustness Bounds by State Transformation," *IEEE Transactions on Automatic Control*, Vol. AC-31, No. 9, pp. 863-866, Sept 1986.
- 7) Horowitz, I., "Quantitative Feedback Theory," *IEE Proceedings*, Vol. 129, Part D, No. 6, pp. 215-226, Nov 1982.
- 8) Kushner, H.J., *Stochastic Stability and Control*, Academic Press, New York, 1967.
- 9) Stengel, R.F., "Some Effects of Parameter Variations on the Lateral-Directional Stability of Aircraft," *AIAA Journal of Guidance and Control*, Vol. 3, No. 2, pp. 124-131, Apr 1980.
- 10) Stengel, R.F. *Stochastic Optimal Control: Theory and Application*, John Wiley and Sons, New York, 1986.
- 11) Siljak, D.D., *Nonlinear Systems, The Parameter Analysis and Design*, J. Wiley & Sons, New York, 1969.
- 12) Ackermann, J., "Parameter Space Design of Robust Control Systems," *IEEE Transactions on Automatic Control*, Vol. AC-25, No. 6, pp. 1058-1072, Dec 1980.
- 13) Putz, P., and Wozny, M.J., "A New Computer Graphics Approach to Parameter Space Design of Control Systems," *IEEE Transactions on Automatic Control*, Vol. AC-32, No. 4, pp. 1058-1072, Apr 1987.
- 14) Boyd, S., Balakrishnan, V., Barratt, C., Khraishi, N., Li, X., Meyer, D., and Norman, S., "A New CAD Method and Associated Architectures for Linear Controllers," *IEEE Transactions on Automatic Control*, Vol. AC-33, No. 3, pp. 268-283, Mar 1988.
- 15) Evans, W.R., "Graphical Analysis of Control Systems," *Transactions of the American Institute of Electrical Engineers*, Vol. 67, pp. 547-551, 1948.
- 16) Doyle, J.C., "Guaranteed Margins for LQG Regulators," *IEEE Transactions on Automatic Control*, Vol. AC-23, No. 4, pp. 756-757, Aug 1978.
- 17) Doyle, J.C., and Stein, G., "Multivariable Feedback Design: Concepts for a Classical/Modern Synthesis," *IEEE Transactions on Automatic Control*, Vol. AC-26, No. 1, pp. 4-16, Feb 1981.